Modeling the Fluid Dynamics of Electro-Wetting on Dielectric (EWOD)

S. Walker[*] and B. Shapiro[**]

[*]University of Maryland, swalker@wam.umd.edu
[**]University of Maryland, benshap@eng.umd.edu

ABSTRACT

By applying voltages across a liquid droplet and an underlying dielectric, it is possible to make dielectric forces compete with surface tension forces, and to thereby cause the liquid droplet to change shape. This effect has been used to successfully move, mix, split, and join droplets in micro-fluidic devices. In our past research we have developed models for the equilibrium deformation of electrically actuated liquid droplet. In this paper, we present a model for the fluid dynamics that can capture the time-varying velocity fields inside the liquid and which can predict the dynamics of droplet splitting and joining. The model runs in minutes, is implemented in Matlab, and is being used to design controllers for precise control of droplet motion and droplet splitting.

Keywords: 2-phase flow, electrowetting, micro-fluidics, modeling, control.

1 INTRODUCTION

Electro-wetting on Dielectric (EWOD) has been demonstrated experimentally in [1-5]. Our goal is to design controllers for the UCLA electro-wetting devices. To do this we need models that are predictive yet whose dimensionality (their number of internal states) is sufficiently low so that they fit into available control design methodologies. Most state-of-the-art control tools can only handle models with thousands to tens of thousands of states, hence it is simply not practical to design controllers using full fledged computational fluid dynamic (CFD) codes containing millions of states. In this paper we present a computational model that predicts the EWOD behavior but that is sufficiently low dimensional to use for control design.

The paper is organized as follows. Section 2 gives a very brief overview of the EWOD devices. Section 3 develops the governing fluid equations. Section 4 outlines the numerical solution scheme. Section 5 closes with some numerical results.

2 DESCRIPTION OF THE DEVICES

A schematic of an EWOD device is shown in Figure 1. The device consists of a top (see through) electrode, droplets of water (here only one droplet is shown), and an underlying grid of electrodes. There is also a layer of hydrophobic Teflon and a layer of solid dielectric silicon dioxide (not shown) between the water and the electrodes. Each electrode effectively changes the surface tension properties above it, and this change can be used to move droplets from electrode to electrode, to split droplets (by pulling on either side using three electrodes), to join droplets by making them collide, and to mix fluid in droplets by making the droplets execute complex paths.
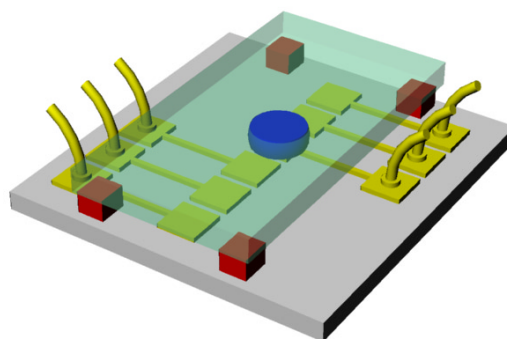

Figure 1: Schematic of sample EWOD device. (Figure courtesy of CJ Kim at UCLA.)

An actual device with a splitting droplet is shown below, the view is through the top (see through) electrode.
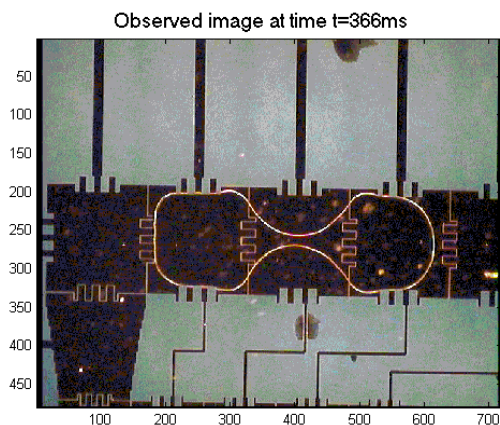

Figure 2: A splitting drop (seen from above) in an EWOD device. (Figure courtesy of CJ Kim at UCLA.)

In [6] we presented a model for the equilibrium shape of droplets under applied electric fields. In this paper, we further consider the non-equilibrium fluid dynamics, specifically; we focus on capturing motion, spliting, and joining of the liquid droplets.

3 GOVERNING FLUID EQUATIONS

Let us begin with the main assumptions used in the fluid flow analysis for the EWOD device. First note that only the liquid is considered; the airflow dynamics are ignored. Since the spacing between the two plates of the device is small compared to the horizontal dimensions, the problem is effectively 2-dimensional. The flow is assumed to be a continuum [7]; this is valid because the Knudsen number is very small due to the density of the liquid and the *relatively* large spacing of the plates (i.e. the channel height is larger than a micron). The flow equations are then derived from the Navier-Stokes equations (see [8], [9]) by making some fairly mild assumptions, such as incompressibility and Poiseuille flow assumptions.
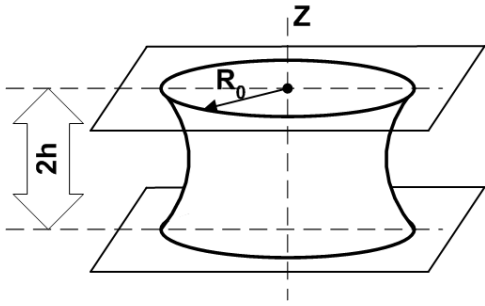

Figure 3: Illustration of EWOD Geometry (with a liquid bridge joining the plates).

Let the X-Y plane (i.e. the Z = 0 plane) be centered between the two plates of the EWOD slab. Let the distance between the plates (i.e. the channel height) be 2h (see Figure 3). Assume that the Z-component of velocity is zero (i.e. w = 0). Assume gravity has a negligible effect; this is valid because the channel height is very small (approximately 10-100 microns). Also, assume that the flow is locally Poiseuille at the point (X, Y) in the plane. Meaning that the X and Y velocity components (i.e. u & v) have a quadratic velocity profile along the Z-axis. Again, this is a good approximation because of the channel height. This puts the fluid equations into the following form:

$$\frac{\partial u}{\partial x} + \frac{\partial v}{\partial y} + \frac{\partial w}{\partial z} = 0$$

$$\rho\left[\frac{\partial u}{\partial t} + u\frac{\partial u}{\partial x} + v\frac{\partial u}{\partial y} + w\frac{\partial u}{\partial z}\right] = -\frac{\partial p}{\partial x} + \mu\left[\frac{\partial^2 u}{\partial x^2} + \frac{\partial^2 u}{\partial y^2} + \frac{\partial^2 u}{\partial z^2}\right] + \rho f_x$$

$$\rho\left[\frac{\partial v}{\partial t} + u\frac{\partial v}{\partial x} + v\frac{\partial v}{\partial y} + w\frac{\partial v}{\partial z}\right] = -\frac{\partial p}{\partial y} + \mu\left[\frac{\partial^2 v}{\partial x^2} + \frac{\partial^2 v}{\partial y^2} + \frac{\partial^2 v}{\partial z^2}\right] + \rho f_y$$

$$\rho\left[\frac{\partial w}{\partial t} + u\frac{\partial w}{\partial x} + v\frac{\partial w}{\partial y} + w\frac{\partial w}{\partial z}\right] = -\frac{\partial p}{\partial z} + \mu\left[\frac{\partial^2 w}{\partial x^2} + \frac{\partial^2 w}{\partial y^2} + \frac{\partial^2 w}{\partial z^2}\right] + \rho f_z$$

Where u, v, and w are given as:

$$\begin{bmatrix} u(x,y,z) \\ v(x,y,z) \\ w(x,y,z) \end{bmatrix} = \begin{bmatrix} u_{ave}(x,y) \\ v_{ave}(x,y) \\ 0 \end{bmatrix}\phi(z), \quad \phi(z) = \frac{3}{2}\left[1 - \left(\frac{z}{h}\right)^2\right]$$

The function $\Phi(z)$ is chosen so that its average over the plate spacing is 1. After integrating along the Z-direction, and performing some algebra, we get the equations into the form:

$$\frac{\partial u_{ave}}{\partial x} + \frac{\partial v_{ave}}{\partial y} = 0$$

$$\rho\left[\frac{\partial u_{ave}}{\partial t} + 1.2\left(u_{ave}\frac{\partial u_{ave}}{\partial x} + v_{ave}\frac{\partial u_{ave}}{\partial y}\right)\right] = -\frac{\partial p}{\partial x} + \mu\left[\frac{\partial^2 u_{ave}}{\partial x^2} + \frac{\partial^2 u_{ave}}{\partial y^2} - \frac{3}{h^2}u_{ave}\right]$$

$$\rho\left[\frac{\partial v_{ave}}{\partial t} + 1.2\left(u_{ave}\frac{\partial v_{ave}}{\partial x} + v_{ave}\frac{\partial v_{ave}}{\partial y}\right)\right] = -\frac{\partial p}{\partial y} + \mu\left[\frac{\partial^2 v_{ave}}{\partial x^2} + \frac{\partial^2 v_{ave}}{\partial y^2} - \frac{3}{h^2}v_{ave}\right]$$

Where the following boundary condition can be derived from the Young-Laplace relationship (see reference [10]):

$$p(\partial\Omega) = \sigma_{lg}\left[\underbrace{K_{xy}(\partial\Omega) + \frac{1}{h}\cos\theta_0}_{mean\ curvature} - \frac{1}{h}\frac{Cap_{area}}{2\sigma_{lg}}Volt^2(\partial\Omega)\right]$$

Where,

- $\partial\Omega$ is the boundary (in the X-Y plane) defined by the liquid/gas interface of the droplet.
- $K_{xy}(\partial\Omega)$ is the curvature of the boundary in the X-Y plane.
- θ_0 is the nominal contact angle of the droplet with the dielectric solid.
- $\frac{1}{h}\cos\theta_0$ is an approximation of the boundary's curvature in the Z-direction.
- The *mean curvature* is just the sum of the two *principal curvatures* (one in the X-Y plane, the other parallel to the Z-axis).
- $Volt(\partial\Omega)$ is the voltage applied to the electrode at a particular point of the boundary.
- σ_{lg} is the surface tension of the liquid/gas interface.
- Cap_{area} is the total capacitance per unit area in the solid dielectric layer.
- μ is the dynamic viscosity of the liquid.

- ρ is the density of the liquid.

Since any *constant* offset to the pressure function does not change the velocity distribution in the droplet, we can rewrite the boundary condition as:

$$p(\partial\Omega) = \sigma_{\mathrm{lg}}\left[K_{xy}(\partial\Omega) - \frac{1}{h}\frac{Cap_{area}}{2\sigma_{\mathrm{lg}}}Volt^2(\partial\Omega) \right]$$

Now perform a non-dimensionalization with the following length scales:

- Length Scale: L = electrode length.
- Velocity Scale: U_0 = maximum velocity of a fluid droplet.
- Pressure Scale: $p_0 = \sigma_{\mathrm{lg}}/L$.
- Time Scale: $t_0 = L/U_0$.

This gives the following dimensionless terms:

- $\widetilde{x} = x/L$, $\widetilde{y} = y/L$.
- $u = u_{ave}/U_0$, $v = v_{ave}/U_0$.
- $\widetilde{p} = p/p_0$.
- $\widetilde{t} = t/t_0$.
- $\widetilde{K}_{xy} = K_{xy}\cdot L$ (dimensionless curvature).

This gives the dimensionless equations (note: the '~' is dropped for simplicity):

$$\frac{\partial u}{\partial x} + \frac{\partial v}{\partial y} = 0$$

$$\mathrm{Re}\begin{bmatrix}\dfrac{\partial u}{\partial t}\\[1ex]\dfrac{\partial v}{\partial t}\end{bmatrix} = -\frac{1}{Ca}\begin{bmatrix}\dfrac{\partial p}{\partial x}\\[1ex]\dfrac{\partial p}{\partial y}\end{bmatrix} + \begin{bmatrix}\nabla^2 u - 3\left(\dfrac{L}{h}\right)^2 u\\[1ex]\nabla^2 v - 3\left(\dfrac{L}{h}\right)^2 v\end{bmatrix}$$

$$p(\partial\Omega) = K_{xy}(\partial\Omega) - \frac{L}{h}F(\partial\Omega, t)$$

Where the bulk convective momentum terms have been dropped because of small Reynolds numbers at the micro-scale. However, the time derivative is kept in to account for rapidly changing boundary conditions induced by high frequency voltage actuation. Also, F, Re, and Ca are defined as:

- $F(\partial\Omega, t) = \dfrac{Cap_{area}}{2\sigma_{\mathrm{lg}}}Volt^2(\partial\Omega)$ (note: F is dimensionless).

- $\mathrm{Re} = \dfrac{\rho L U_0}{\mu}$, $Ca = \dfrac{\mu U_0}{\sigma_{\mathrm{lg}}}$.

4 NUMERICAL SOLUTION SCHEME

Simulating EWOD droplet behavior requires that the droplet boundaries be properly defined. This is achieved by using a level set method ([11], [10], [12], [13]) which effectively captures the liquid-gas interface as the zero level set of a scalar function defined on the X-Y plane. Using this, the pressure and velocity fields inside the droplet can be obtained by finite difference methods. The velocity field is then used to update the scalar level set function. The motion of the droplet is ultimately captured by the evolution of the zero level set of the scalar function. A summary of the algorithm is given here:

0. Initialization: A Cartesian computational grid defined on a unit square is used to sample the level set and solve for the fluid variables. The scalar level set function is initialized to be a distance function with a zero level set corresponding to the initial shape of the droplet. The level set is chosen to be positive on the domain where the liquid is, and is negative elsewhere.

1. Pressure Field: Laplace's equation with Dirichlet boundary conditions is used to solve for the pressure field. The interior solution domain is given by where the level set function is positive. The boundary conditions are applied at the grid notes adjacent to the interior domain nodes, and are computed based on the local interface curvature and applied voltage. The interface curvature is calculated using standard 2nd order central difference formulas operating on the level set function φ. The solution scheme is based on a multi-grid Jacobi iterative solver.

$$\Delta p = 0, \quad p(\partial\Omega) = K_{xy}(\partial\Omega) - \frac{L}{h}F(\partial\Omega, t)$$

$$K_{xy} = -\frac{\phi_x^2\phi_{yy} - 2\phi_x\phi_y\phi_{xy} + \phi_y^2\phi_{xx}}{\left(\phi_x^2 + \phi_y^2\right)^{3/2}}$$

2. Velocity Field: Through the use of a stream-function formulation, and a discrete Fourier transform technique, the velocity field is obtained for the current time step.

$$\frac{\partial u}{\partial x} + \frac{\partial v}{\partial y} = 0$$

$$\mathrm{Re}\begin{bmatrix}\dfrac{\partial u}{\partial t}\\[1ex]\dfrac{\partial v}{\partial t}\end{bmatrix} = -\frac{1}{Ca}\begin{bmatrix}\dfrac{\partial p}{\partial x}\\[1ex]\dfrac{\partial p}{\partial y}\end{bmatrix} + \begin{bmatrix}\nabla^2 u - 3\left(\dfrac{L}{h}\right)^2 u\\[1ex]\nabla^2 v - 3\left(\dfrac{L}{h}\right)^2 v\end{bmatrix}$$

3. Level Set Update: After adaptively choosing a time step that obeys the CFL condition, the level set function is updated through a convection-type equation using a Hamilton-Jacobi WENO method. $\phi_t + u\phi_x + v\phi_y = 0$

4. Loop: Go to step 1, and solve using the updated level set function. Iterate this process as long as necessary.

5 RESULTS

The simulation was tested for the same on/off/on electrode case that is shown in the experiment of Figure 2. The sequence of figures below shows the attained results. When these figures are overlaid with the experiment, it can be seen that the simulation accurately matches the experiment.
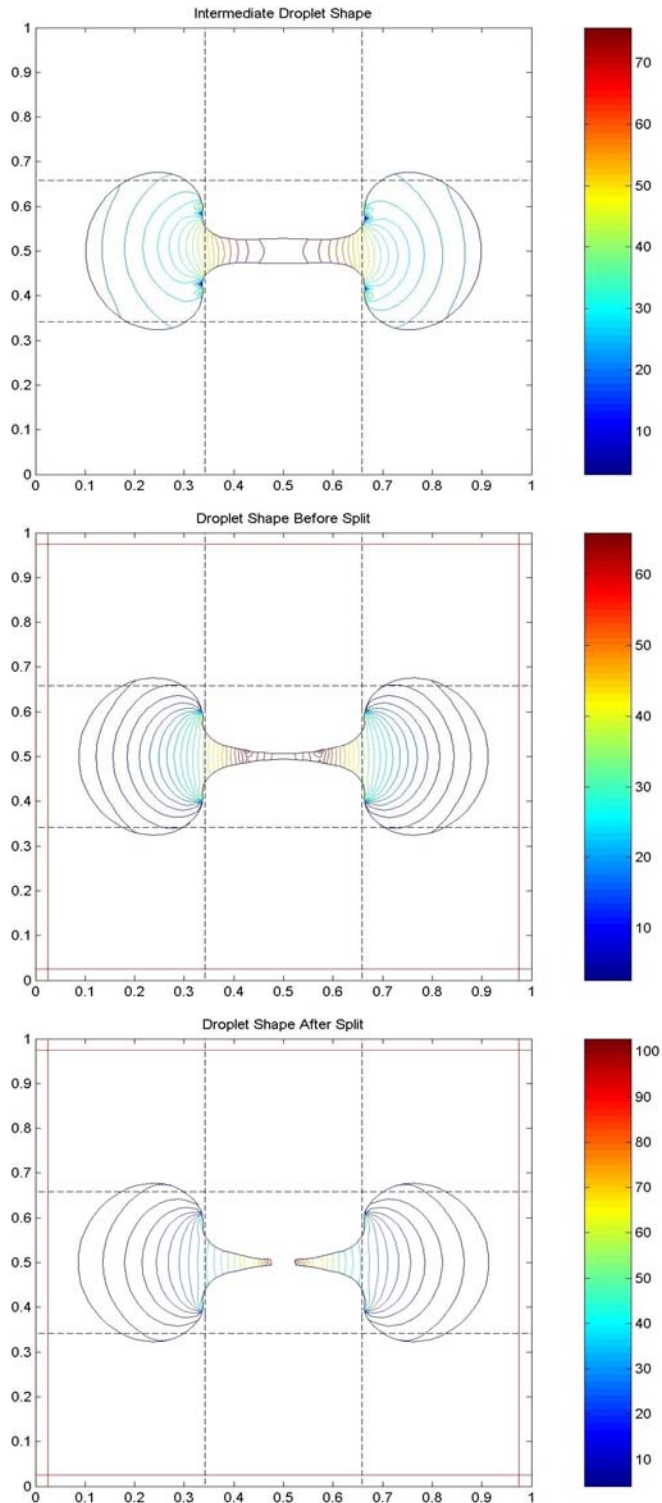

Figure 4: Numerical results for droplet splitting. The simulation corresponds to the electrode on/off/on case used in Figure 2. Each electrode is of x width 1/3rd and of unit y length. The colored curves correspond to the pressure contours inside the liquid droplet.

REFERENCES

[1] C. J. Kim and J. Lee, "Microactuation by Continuous Electrowetting Phenomenon and Silicon Deep RIE Process," presented at ASME Int. Mechanical Engineering Congress and Exposition, Anaheim CA, 1998.

[2] C. J. Kim and J. Lee, "Liquid Micromotor Driven by Continuous Electrowetting," presented at IEEE Micro Electro Mechanical Systems Workshop, Heidelberg, Germany, 1998.

[3] M. Vallet, B. Berge, and L. Vovelle, "Electrowetting of water and aqueous solutions on poly(ethyleneterephthalate) insulating films.," *The European Physical Journal*, vol. 11, pp. 583-591, 1996.

[4] E. Seyrat and R. A. Hayes, "Amorphous fluoropolymers as insulators for reversible low-voltage electrowetting," *Journal of Applied Physics*, vol. 90, 2001.

[5] H. J. J. Verheijen and W. J. Prins, "Reversible electrowetting and trapping of charge: Model and experiments.," *Langmuir*, vol. 15, pp. 6616-6620, 1999.

[6] B. Shapiro, H. Moon, R. Garrell, and C. J. Kim, "Equilibrium Behavior of Sessile Drops under Surface Tension, Applied External Fields, and Material Variations," *Journal of Applied Physics*, vol. 93, 2003.

[7] G. E. Karniadakis and A. Beskok, *Micro Flows: Fundamentals and Simulation*. New York, NY: Springer Verlag, 2001.

[8] R. L. Panton, *Incompressible Flow*, 2 ed. New York, NY: John Wiley & Sons, Inc., 1996.

[9] G. K. Batchelor, *An Introduction to Fluid Dynamics.*: Cambridge University Press., 1967.

[10] S. A. Sethian, *Level Set Methods & Fast Marching Methods*, 2 ed: Cambridge University Press, 1999.

[11] S. Osher and R. Fedkiw, *Level Set Methods and Dynamic Implicit Surfaces.*: Springer-Verlag New York., 2003.

[12] R. P. Fedkiw, T. Aslam, B. Merriman, and S. Osher, "A non-oscillatory eulerian approach to interfaces in multi-material flows (the ghost fluid method)," *Comput. Phys.*, vol. 152, pp. 457-492, 1999.

[13] R. Caiden, R. Fedkiw, and C. Anderson, "Numerical Method for Two Phase Flow Consisting of Separate Compressible and Incompressible Regions," *J. Comput. Phys.*, vol. 166, pp. 1-27, 2001.